Carbohydrate Polymers 103 (2014) 250–260

Contents lists available at ScienceDirect

Carbohydrate Polymers

journal homepage: www.elsevier.com/locate/carbpol

Elucidation of hydration dynamics of locust bean gum–collagen composites by impedance and thermoporometry

Ivy Kanungo, Nishter Nishad Fathima, Raghava Rao Jonnalagadda*, Balachandran Unni Nair

Chemical Laboratory, Central Leather Research Institute, Council of Scientific and Industrial Research, Adyar, Chennai 600020, India

ARTICLE INFO

Article history:
Received 29 August 2013
Received in revised form 9 December 2013
Accepted 14 December 2013
Available online 25 December 2013

Keywords:
Collagen
Locust bean gum
Impedance
Thermoporometry
Hydration

ABSTRACT

The intricacy of the different parameters involved in the hydration dynamics of collagen influences its performance as biomaterials. This work presents the molecular motions of collagen originating from the solvents and locust bean gum (LBG), which reveal the changes in solvation dynamics of the biopolymers affecting the surface as well as interfacial properties. Water, as a probe liquid bound in collagen has been investigated using a combination of thermoporometry, ATR-FTIR, circular dichroic spectroscopy, dielectric spectroscopy and SEM to explore the influence of LBG on collagen with respect to static and dynamic behaviour. The relaxation process of collagen in the frequency range of 0.01 Hz to 10^5 Hz and thermoporometry results indicate that the interfacial hydration dynamics are dependent on the applied concentration of LBG. This investigation explicitly reflects the rearrangements of the structural water clusters around the charged amino acids of collagen. These results can be employed to redesign the approach towards the development of collagen based biomaterials.

1. Introduction

Polysaccharides, the natural polymeric materials, have diverse set of functions. They play a well-known function as a reserved material in membranes utilized during germination (Prajapatia, Jani, Moradiya, Randeria, & Nagar 2013) and intracellular communication, while proteins function as structural materials and catalysis (Dionisio & Grenha, 2012). The current trend in the tissue engineering application is to mimic nature, leading to exploration of natural biopolymer in the biomedical and biopharmaceutical applications. The notion of polysaccharides is equally interesting in the design of nanostructured biomaterials (Rinaudo, 2008).

Locust bean gum (LBG), a non-starch natural polysaccharide consisting of galactose and mannose in the ratio 1:4 (Structure given as supplementary data Fig. S1), has a wide application in tissue engineering and pharmaceuticals due to their tailorable physico-chemical properties (Parvathy, Susheelamma, Tharanathan, & Gaonkar, 2005; Prajapatia et al., 2013). LBG is highly viscous, nonionic polymer, which is unaffected by variations in pH, salinity and temperature (Kaity & Ghosh, 2013; Kaity, Isaac, Mahesh Kumar, et al., 2013). The relative hydrophobicity of mannose permits the formation of strong intra-molecular hydrogen bonds, having a propensity to form aggregates in cold water due to the reduction of hydration of gums. The strong synergistic interaction of LBG with other polysaccharides is attributed to the numerous —OH groups, which results in the gelling structure for biopharmaceutical applications (Dakia, Wathelet, & Paquot, 2007; Kaity, Isaac, & Ghosh, 2013; Wang & Somasundaran, 2007).

Collagen based biomimetic scaffolds have made a great strides in the field of tissue engineering. Fibrillary collagen, one of the most abundant structural proteins present in the extracellular matrix (ECM), permits the incorporation of known biological signals recognized by the receptors and other intracellular proteins. A number of important aspects that determines the performance of biomimetic scaffolds include the composition, structure and mode of processing performed. Biomaterials designed to have specific dimensions, interfacial structure, hydration dynamics, interconnectivity and surface chemistry could in principle emulate the architectural features and cell signalling machinery of the natural extracellular matrices to promote regenerative medicinal application. Presence of higher polar groups such as carboxyl, hydroxyl or amine groups results in more polarity and higher wettability. Due to this fact, the controlled modification of polarity, hydrophobicity and charge becomes a complicated process for intended biomedical application (Desmet et al., 2009). The understanding of the interfacial or surface structure of the biomaterials and its relation to the macroscopic properties has proven to be an extremely valuable tool to comprehend the cell adhesion mechanism at molecular level. The orientation of water bridges influences the short and long range intermolecular interactions. The energetic contribution of

* Corresponding author. Tel.: +91 44 24411630; fax: +91 44 24911589.
E-mail addresses: clrichem@mailcity.com, jrrao@clri.res.in (J. Raghava Rao).

0144-8617/$ – see front matter © 2014 Elsevier Ltd. All rights reserved.
http://dx.doi.org/10.1016/j.carbpol.2013.12.051

attractive hydration forces arising from water bridges is an interesting but often neglected aspect of macromolecular interactions. The hydration dynamics of protein is greatly influenced by the co-solutes such as cross-linkers (Farrist, Song, & Huang, 2009). Genipin, extracted from *Gardenia jasminoides* Ellis, is one of the crosslinking agents for proteins and polysaccharides (O'Brien, Harley, Yannas, & Gibson, 2005). Glutaraldehyde is the most widely used cross-linker for stabilizing collagen, but of recently, several reports demonstrate that genipin is about 10,000 times less cytotoxic compared to glutaraldehyde and is also biocompatible (Nishi, Nakajima, & Ikada, 1995). Crosslinking of collagen with genipin involves nucleophilic attack by primary amine groups of lysine or hydroxylysine amino acids residues of the polypeptide chains at the C3 carbon atom in genipin (Yoo, Kim, Kim, & Choi, 2011). Thereafter, Schiff base is formed leading to subsequent reactions that may be involved in the intramolecular and intermolecular crosslinking of collagen.

This work focuses on the understanding the hydration dynamics and designing of collagen–locust bean gum based composites crosslinked with genipin. As represented in Fig. 1, the designer materials facilitate multiple noncovalent as well as covalent interactions resulting in modulation of hydration dynamics of collagen. Dielectric techniques (Kandamchira, Kanungo, & Fathima, 2012) have been previously used to study the effect of water and electric field frequencies on the dielectric properties of constituent phases of collagen. Impedance measurement gives the molecular insights into the dipole–dipole interaction and hydration dynamics at the collagen–additives interfaces (Friess & Lee, 1996; Manikoth, Kanungo, Fathima, & Rao, 2012; Marzec & Warchol, 2005; Samouillan, Lamure, & Lacabanne, 2000; Samouillan, Lamureet al., 2000). Thermoporometry utilizes the traditional differential scanning calorimetric technique in an untraditional way to quantify water in nanoscale pores (Fathima, Baias, Blumich, & Ramasami, 2010; Fathima, Pradeepkumar, Rao, & Nair, 2010). In view of the above, the structural characteristics of water sorbed in the pores of the collagen–LBG composites are investigated using dielectric measurements, thermoporometry, circular dichroic spectroscopy, ATR-FTIR spectroscopy for the development of new biomaterials.

2. Experimental

2.1. Materials

Frozen rat tail tendon (RTT), excised from 6 month old albino rats (Wistar strain) were thawed and teased out. Locust bean gum (M_w ~310 kDa), genipin and picrylsulfonic acid [2,4,6-trinitrobenzene sulfonic acid (TNBS)] were purchased from Sigma–Aldrich. Water used for these studies was of millipore grade.

2.2. Isolation and collagen type I solution preparation

Tails of 6 month old male albino rats (Wistar strain) were excised due to its high purity, available lysine residues suitable for crosslinking and frozen at 253 K. The collagen type I solution was prepared after washing the teased collagen fibre with 0.9% NaCl at 277 K by acetic acid extraction method and salting out with NaCl (Chandrakasan, Torchia, & Piez, 1976). SDS-PAGE technique was employed to estimate the purity of extracted collagen. The collagen concentration in the solution was determined from the hydroxyproline content according to the method of Woessner (1961). A factor of 7.2 was used for calculating the mass ratio of collagen to hydroxyproline. The average molecular weight of

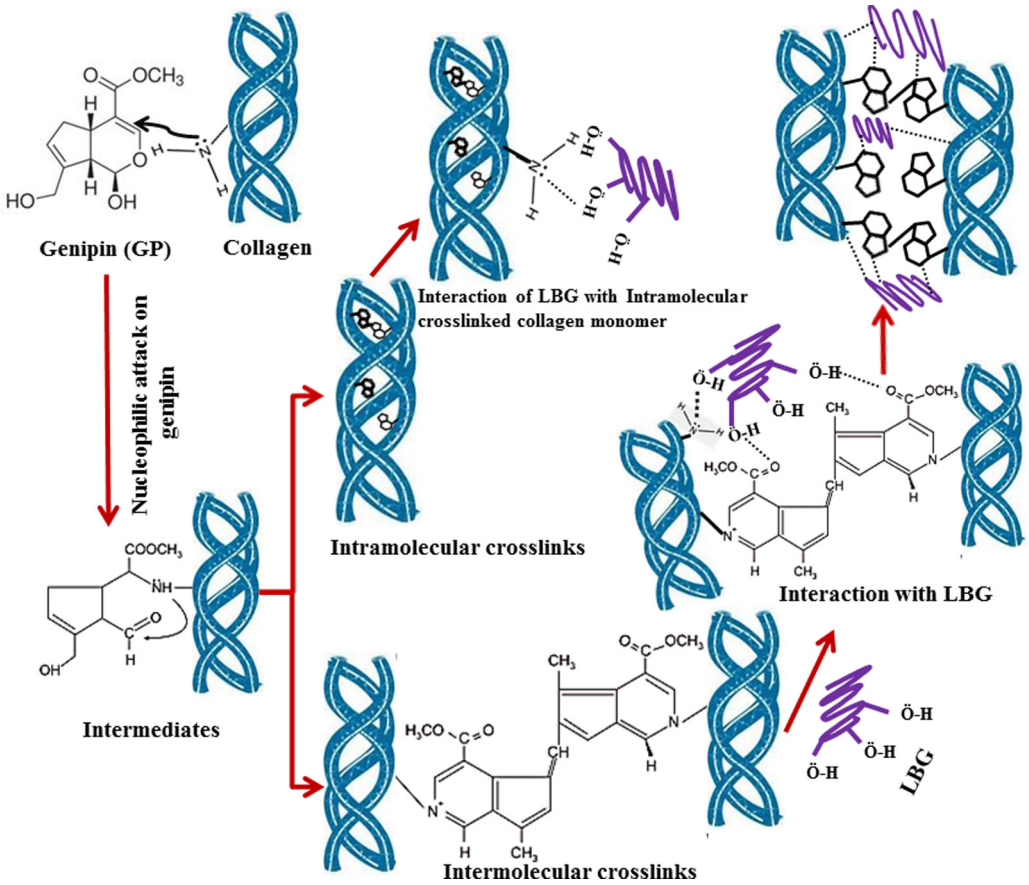

Fig. 1. Schematic representation of interaction of genipin crosslinked collagen–locust bean gum (LBG) composites interconnected with intra- and intermolecular hydrogen bonded network.

collagen is 300,000 Da (Ramachandran, 1967) based on which the molar concentration was determined.

2.3. Preparation of collagen–locust bean composites

The locust bean gum (LBG) was dissolved in water by heating it to about 353 K for 4 h. Prior to mixing with collagen, LBG solution was cooled down to room temperature. Collagen (0.5 μM) and LBG solution were mixed in acetate buffer of pH 4.2 in different molar ratios viz. 2:1 (C-COLLBG-1), 1:1 (C-COLLBG-2), 2:3 (C-COLLBG-3) and 1:2 (C-COLLBG-4) under stirring condition for 2 h at 277 K. In situ hydration in acid aqueous environment was applied in this work to obtain a homogenous composite solution. The composites were further stirred for 3 h to stiffen the network using genipin (0.05 wt% of collagen) as the crosslinking agent. The samples were lyophilized under the pressure of 48 mtorr at 233 K for SEM and ATR-FTIR analysis.

2.4. Circular dichroic spectral acquisition of system

CD spectra were recorded in the UV range 190–260 nm using a rectangular quartz cells with an optical path 0.1-cm path on a Jasco-815 spectropolarimeter with collagen concentration of 0.5 μM at 298 K. Each spectrum was the accumulation of three scans followed by noise reduction. Influence of LBG on the temperature induced conformational changes of collagen was studied at the pH of 4 at a temperature range of 309–315 K and an interval of 0.5 K under N_2 atmosphere.

2.5. ATR-FTIR spectral acquisition of collagen–LBG composites

ATR-FTIR spectra were recorded on an ABB MB 3000 (Pike Technologies, USA) infrared spectrometer over the spectral range of 4000–600 cm^{-1}, with a resolution of 4 cm^{-1} at 298 K. 21 scans were averaged for each spectrum. The background spectrum of air was subtracted from the sample spectra using the software HORIZON MB™. The interferogram was transformed into sample ATR-FTIR Spectra.

2.6. Thermoporometric analysis

Thermoporometric analysis was carried out using TA Instruments Q200 Differential Scanning Calorimeter (DSC), USA in a temperature range from 233 to 283 K at a heating rate of 1 K/min under nitrogen atmosphere. The stability of the baseline was checked before each measurement. Prior to measurement, the liquid test sample sealed in hermetically encapsulated aluminium pan was cooled to 233 K and held at that temperature for 30 min. The peak transition temperature (T_m) and total enthalpy (H_m) for the transition was obtained using the system generated software. All the measurements were performed in triplicates and mean value was reported. The pore size distribution was calculated as described earlier (Kanungo, Chellappa, Fathima, & Rao, 2011; Kanungo, Fathima, Rao, & Nair, 2013a; Manikoth et al., 2012).

2.7. Polarimetric data acquisition of collagen–LBG composites

The dielectric properties of the composite solutions were measured in the frequency range from 0.01 to 10^5 Hz, at 298 K by means of three electrode systems in a CH Instrumental (USA) electrochemical analyzer CH-model 660B, where the glassy carbon electrode was used as a working electrode, a platinum electrode as a counter electrode and a saturated calomel electrode as the reference electrode. All the experiments were done in triplicate and the mean was reported.

2.8. Surface imaging of collagen–LBG composites

SEM (Hitachi S-3400 (Japan)), with an accelerating voltage of 15 kV) was used for the imaging of the fracture surfaces of the lyophilized sample, which were kept on one side of the adhesive stub to be coated with gold using sputter coater (JEOL-JFC 1600 AUTO COATER).

2.9. Determination of degree of crosslinking

The crosslinking degree of the genipin-crosslinked collagen–LBG composites was determined by 2,4,6-trinitrobenzenesulfonic acid (TNBS) assay that determines the ε-amino groups in collagen. Crosslinking degree was assessed by measuring the available free lysine and comparing free lysine content before and after crosslinking using TNBS. Prior to the assay, TNBS was prepared in acetate buffer. 500 μl native collagen (0.5 μM) (uncrosslinked) as well as composite samples were mixed with 500 μl 4% $NaHCO_3$ and 0.5% 500 μl of TNBS solution. The samples were subjected for incubation at 313 K for 4 h in dark. Afterwards, 2 ml 6 N HCl was added to the sample-TNBS mixture to stop the reaction. The reaction mixture was kept at 333 K typically for 1 h. The resulting solution was diluted by deionized water. The amount of free ε-amino groups in the test sample was determined by the optical absorbance of the solution recorded after dilution at 345 nm with a spectrophotometer (Model Shimadzu 1800) using acetate buffer as blank. Degree of crosslinking was defined as the ratio of the consumed ε-amino groups in the cross-linked samples to the free ε-amino groups in the native uncrosslinked collagen samples and calculated as follows (Jayakumar et al., 2012; Zhou, Zhang, Ma, & Tong, 2008):

$$\text{Degree of crosslinking } (\%) = \frac{\text{Absorbance of native collagen} - \text{Absorbance of genipin interacted composite system}}{\text{Absorbance of native collagen}} * 100 \quad (1)$$

3. Result and discussion

The composites of LBG and collagen are termed as COLLBGs. Furthermore, these COLLBGs were crosslinked with genipin to obtain C-COLLBGs. LBG mediated noncovalent interactions and genipin mediated covalent interactions result in changes in the structure and dynamics of water at the interfaces affecting protein's structural stability. These have been confirmed by ATR-FTIR spectroscopy, impedance measurement, and circular dichroic spectroscopy.

3.1. Dichroic spectral features of collagen

Circular dichroic spectroscopic studies have been employed to monitor the alteration in the secondary structure of collagen due to interaction with LBG. The overall spectra of all the collagen–LBG composites are similar to CD spectra of polyproline type II (Fig. 2a–e). In the far UV region, the (190–240 nm) CD spectrum of collagen type I measured at 298 K exhibits bands at 197 and 220 nm with a cross over at 210 nm, which are certainly attributable to the characteristic secondary structure of collagen (Fathima, Bose, Rao, & Nair, 2006). The triple helical structure of collagen was confirmed in the complex by its minimum at 197 nm and maximum at 220 nm in the far UV region (figure given as supplementary data

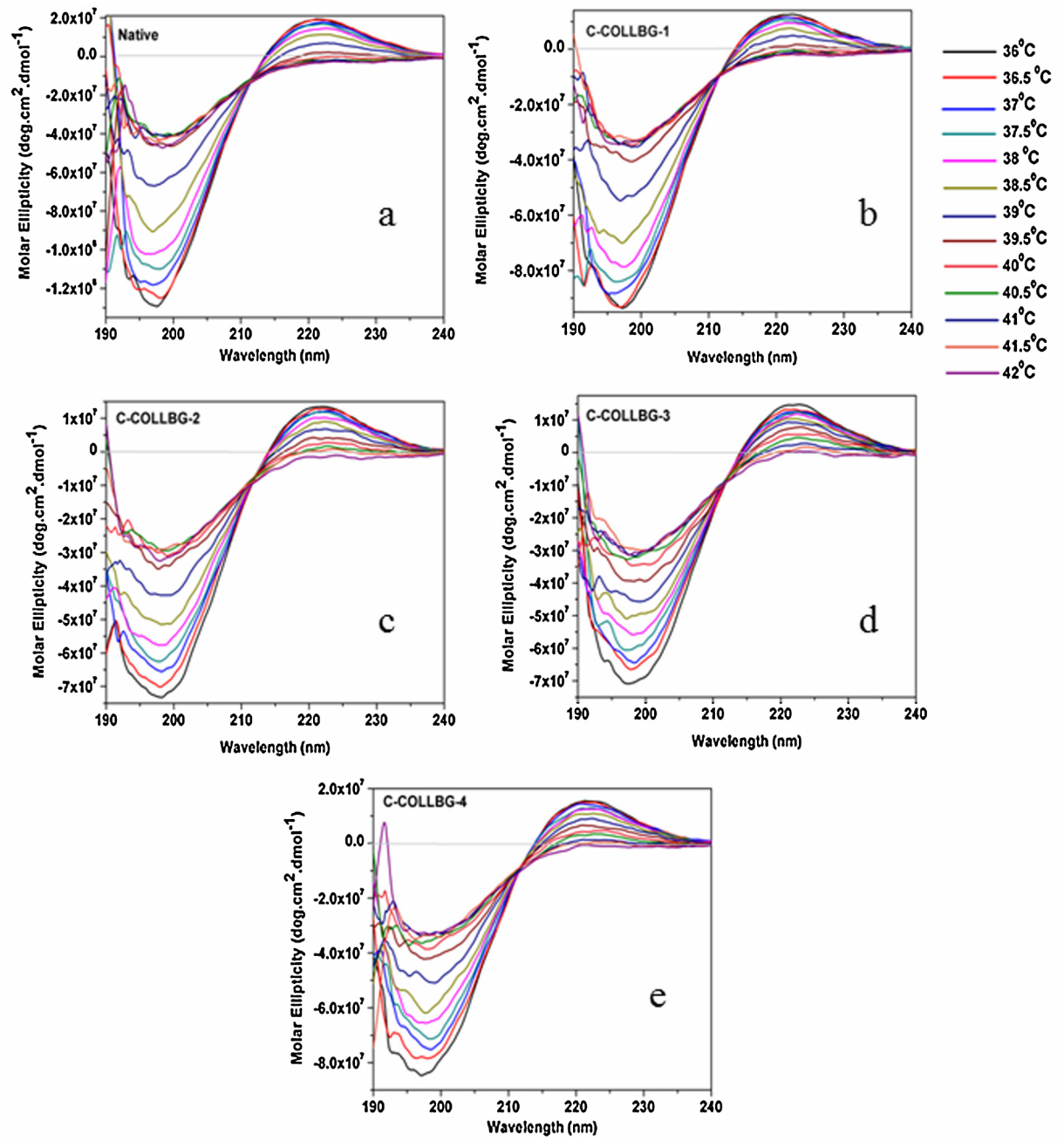

Fig. 2. Temperature dependent circular dichroic spectroscopic measurement various locust bean gum (LBG) concentrations. CD spectra over the range 190–240 nm were recorded in the absence as well as in the presence of LBG.

Fig S2). Thus, it can be inferred that LBG does not alter the secondary structure of collagen. CD band position of collagen at 220 nm is found to be independent of LBG concentration as well as temperature. However, interaction of LBG and genipin with collagen changed the CD band intensities in this region, which were greatly influenced over the range of the LBG concentration. The molar ellipticity values at 220 nm at different concentration range of LBG and at varying temperature range are shown in Fig. 3a.

The ratio of the positive peak over negative peak (Rpn), a characteristic feature of the triple helical conformation of collagen and collagen like peptide (Fathima, Balaraman, Rao, & Nair, 2003; Fathima, Balaraman, Rao, Nair, & Ramasami, 2004) possess a large variation over the LBG concentration at varying temperature range (Fig. 3b). This confirms the strong interaction of LBG on the surface of collagen by close proximity of various functional groups. The intermolecular interaction leads to formation of hydrogen bonding network within the composite matrix raising the thermal stability of collagen to 3%.

3.2. IR spectral features of collagen as affected by additives

Attenuated Total Reflectance Fourier-transform infrared (ATR-FTIR) spectroscopy is a rapid and a non-destructive technique to investigate the interaction between the chemical groups at the molecular level of protein-polysaccharide (Turquois, Acquistapace, Vera, & Welti, 1996). The interaction between the chemical groups at the molecular level indicates the changes in the spectra by shifting of absorption bands (Xu, Li, Kennedy, Xie, & Huang, 2007). ATR-FTIR spectra were scanned over the wavenumber range of 3600–400 cm^{-1}.

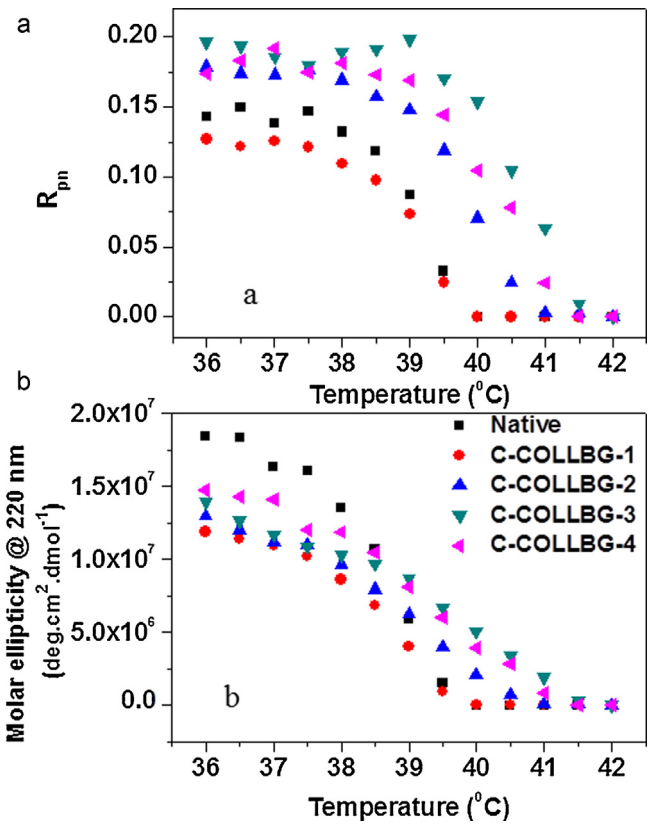

Fig. 3. The unfolding of collagen treated with various locust bean gum (LBG) concentrations. (a) Unfolding monitored by the characteristic R_{pn} value (ratio of positive molar ellipticity value at 220 nm and negative molar ellipticity value at 197 nm). (b) Unfolding monitored by changes of molar ellipticity at 220 nm. The positive molar ellipticity value of completely denatured collagen is considered as 0.

The ATR-FTIR spectrum of pure collagen shows (Fig. 4) the characteristic functionality peaks of amide A (3317 cm^{-1}), amide B (3080 cm^{-1}), amide I (1647 cm^{-1}, C=O stretching), amide II (1552 cm^{-1} N—H bending and C—N stretching), and amide III (1243 cm^{-1}, C—N stretching and N—H bending) (Kanungo, Fathima, Rao, & Nair, 2013b). The peak at a frequency of 2880 cm^{-1} is due to the aliphatic side chains present in the collagen. The broadband ranging between 3600 and 3100 cm^{-1} is attributed to O—H stretching vibration formed by the hydroxyl group of polysaccharides as well as collagen and water. The broadband around 2800–3000 cm^{-1} is attributed to C—H stretching vibration of pure locust bean gum (Cerqueira et al., 2011). ATR-FTIR spectra of our samples also show a band in the region of 750–1300 cm^{-1} that corresponds to the carbohydrates region (Fig. 4). These wavenumbers are within the so-called fingerprint region, where the bands are specific for each polysaccharide, allowing its possible detection (Sen & Erboz, 2010). For COLLBG the band at 2924 cm^{-1} represents C—H stretching of the $-CH_2$ groups, which confirms the presence of LBG. The band due to ring stretching of galactose and mannose of LBG appears at 1657 cm^{-1}. Moreover, the bands in the region of 1350–1450 cm^{-1} show the symmetrical deformations of the CH_2 and C—OH groups. The bands representing the primary alcoholic $-CH_2OH$ stretching mode and CH_2 twisting vibrations appear at 1078 and 1024 cm^{-1}, respectively. The peak around 3300–3600 cm^{-1} indicates the stretching of both phenolic hydroxyl group of LBG as well as aliphatic hydroxyl and amino group of collagen. The little shift of peak from 3320 to 3415 cm^{-1} indicates the change in stretching vibration mode of phenolic hydroxyl group of LBG as well as aliphatic hydroxyl group of collagen. This might be attributed to the formation of hydrogen bond between free NH group of collagen and OH group of the LBG. Since the C-COLLBG-1 shows lower porosity than C-COLLBG-2 and C-COLLBG-3, it is likely that the increase in concentration of LBG leads to increase in crosslinking through hydrogen bonds. Therefore, the transmittance intensity of the —OH bonds is less that of the bonds formed by two other C-COLLBG composites. Fragments of the long chain LBG promote the interactions among the chains leading to the formation of intermolecular hydrogen bonds and van der Walls forces. The degree of the hydrogen bonding increases as a function of LBG concentration, resulting in tightening of the network structure. The change in the intensity of transmittance (%T) peak at 1647 and 1552 cm^{-1} indicates that the carboxymethyl group of genipin has reacted with the ε-amino group of collagen. The peak at 1413 cm^{-1} (C=C stretch) also indicates the formation of cross-linking between the collagen and genipin, and presence of LBG moiety. Notably, the peak at 1241 cm^{-1} (C—N stretching) in the collagen spectrum was completely suppressed in the case of all cross-linked composites, which is due to formation of imidazolium ions. This study clearly represents how the presence of several hydroxyl groups in the LBG molecule influences the possibility of noncovalent multipoint interaction with collagen as well as genipin.

3.3. Polarimetric spectral feature of collagen–LBG composites

The collagen solutions with different concentrations of LBG were subjected for impedance measurement to determine the response of composites to the root-mean-square (rms) amplitude over the range of frequencies, as shown in Fig. 5. Since LBG is constituted by numerous polar groups (—OH) and collagen contains polar repeating units of amino-acid (—CO—CHR—NH—), the dielectric technique is particularly sensitive to analyze the dynamic characteristics of water. Relaxation strength and distribution parameters of relaxation curve are informative tools to pattern the hydrophilicity of the composites. The dielectric relaxations are described by the means of Bode function, which is one of the mostly used relationships to take into account the dielectric relaxations of polymer solutions. The complex impedance of the sample is denoted by

$$Z = Z\prime + jZ'' = R + jX \tag{2}$$

where, Z is the complex impedance, Z' is the real part, Z'' is the imaginary part of the complex impedance, R is the resistance, and X is the reactance response to an alternating signal. The magnitude of the complex impedance and the phase angle (θ) include the complex impedance and expressed as Eqs. (3) and (4)

$$|Z(\omega)| = \sqrt{(Z\prime)^2 + (Z'')^2} \tag{3}$$

$$\theta = \tan^{-1}\left(\frac{Z''}{Z\prime}\right) \tag{4}$$

In order to assess the electrode polarization and ionic conduction effects on composites, the complex dielectric impedance and admittance have been widely used (Kanungo et al., 2013a; Manikoth et al., 2012). The complex dielectric impedance and admittance plane is plotted in two different arcs using the real Z' vs. imaginary Z'' and real Y' vs. imaginary Y'' and is shown in Fig. 5a and b. The electrode polarization results from the formation of electric double-layer capacitances with free charge. The interfacial capacitances, originated at the interface of electrode surfaces and dielectric materials, occur by the substantial increase in the complex dielectric permittivity with decrease in frequency at lower frequency range. The composites are made of covalent, van der Waals, and hydrogen bonds. The dielectric behaviour in high-frequency region has been attributed to the Brownian motion of the hydrogen bonds (Yalçın, Coşkun, Okutan, & Öztürk, 2013). The increase of LBG concentration promotes a decrease in the charge

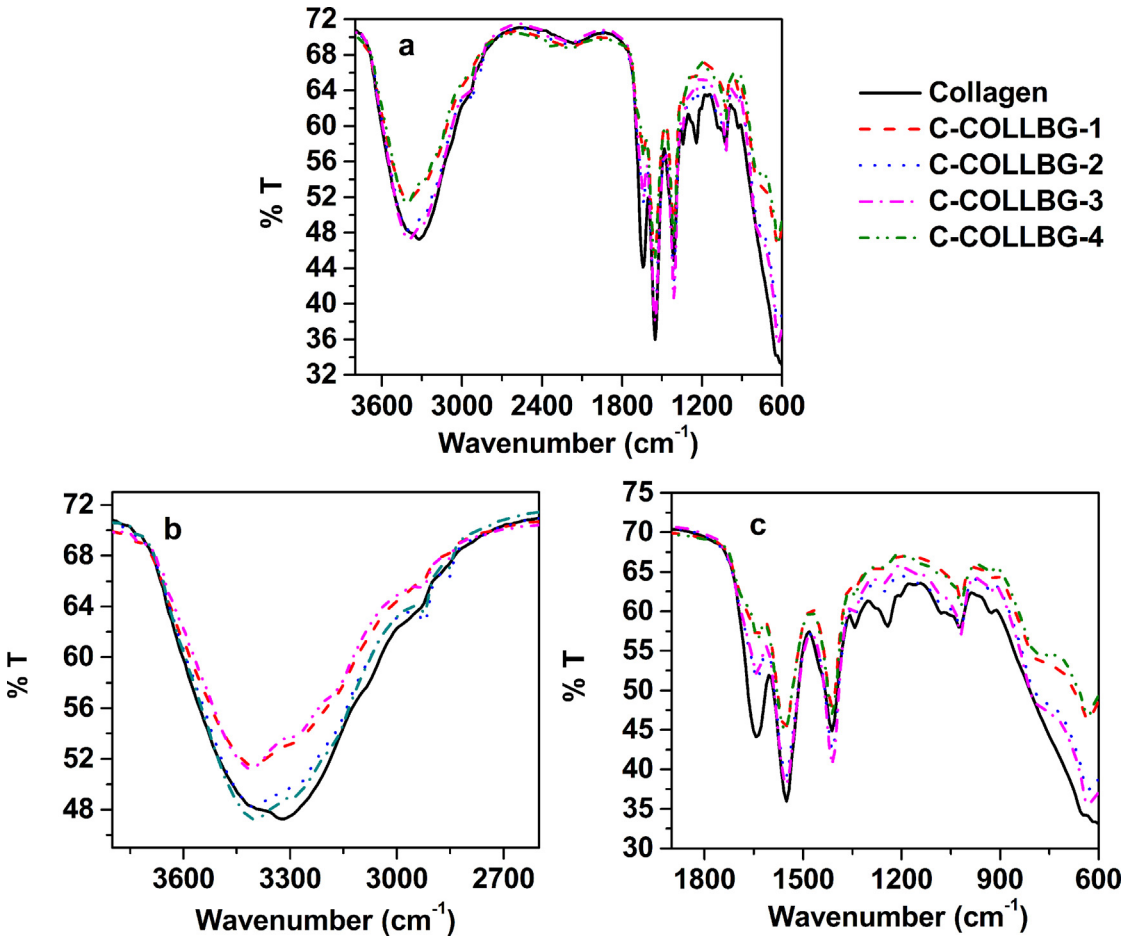

Fig. 4. ATR-FTIR spectra of the collagen and genipin crosslinked collagen–locust bean gum (LBG) composites. (a) Wavenumber: 3800–600 cm^{-1} (b) Wavenumber: 3800–2600 cm^{-1} and (c) Wavenumber: 1900–600 cm^{-1}.

carriers and, consequently, the admittance viz. ionic conductivity up to a limit, which is probably due to the formation of hydrogen bonding with the hydroxyl groups of LBG.

The frequency evolution of the complex impedance for collagen–LBG composites with different LBG concentrations are shown in Fig. 5c. As observed in this figure, all samples show a LBG concentration dependence dispersion behaviour of collagen. This low frequency behaviour for all composites originates from the electrode polarization. The addition of nonionic LBG increases the population of —OH molecules in the solution, which consequently affects the ionic diffusion in the whole system. The frequency evolutions of Z for composites with different LBG concentrations (0.25, 0.5, 0.75, 1 μM) are slowly decreasing, while the frequency is increasing. The log–log graph of Frequency and Z for composites with different LBG concentrations depicted in the Fig. 5c demonstrates the logarithmic decrease of Z with frequency up to 10^3 Hz. The impedance for all samples shows linear behaviour above 10^3 Hz frequency. This linear behaviour in the frequency range of 10^3–10^5 Hz originates from the inductance effects. The formation of hydrogen bonds promotes changes in the dielectric response. The faster secondary relaxations of the polysaccharides has been attributed to internal motions within their monomeric units whereas pressure and temperature sensitive slower secondary relaxations has been governed by analogous motions in the form of local chain rotation. γ-relaxation is associated with local motions of two side groups —CH_2OH and —OH (Kaminski et al., 2009). The real Z' increases as the LBG concentration increases, but a completely opposite result has been seen for C-COLLBG-3. The LBG concentration effect on the phase angle in the frequency range of 0.01 to 10^5 Hz is shown in Fig. 5d. This observation implies that the collagen:LBG molar ratio is critical for achieving the desired hydration property. The results indicate that all the composites exhibit similar phase angle behaviour. The dielectric loss tangent/dissipation factor (Fig. 5e) for collagen–LBG composites with different LBG concentrations has been calculated using this equation,

$$\tan\delta = \frac{Z'}{-Z''} = \tan(90^\circ - \theta) \quad (5)$$

The dissipation factor increases with an increase in frequency as well as LBG concentration. The maximum values of the energy loss factor 9.58 for C-COLLBG-1 and 19.84 for C-COLLBG-4 have been observed at 4826 and 8756 Hz, respectively. The broadening of the maximum peak of the C-COLLBG-4 is attributed to the change in the molecular vibration to rotational motion (Yalçın et al., 2013). The dissipation factor i.e. tan δ and maximum peak frequency values of the samples are listed in Table 1.

This opposite dielectric behaviour recorded for C-COLLBG-3 originated from the strong dependence on the LBG concentrations in composites. It is anticipated that this fact is due to the common motion of LBG–water molecules through hydrogen bonds. Increase in the hydrogen bond density leads to a more localized cooperative mobility (Jafarpour, Roig, Dantras, Boudet, & Lacabanne, 2009). This observation supports the IR spectroscopic data obtained for these composites.

The stabilization through delocalisation of electrons results in the restricted N—C bond rotation. The energy of the H bonded polypeptide chains is lowered. The restricted bond rotation elevates

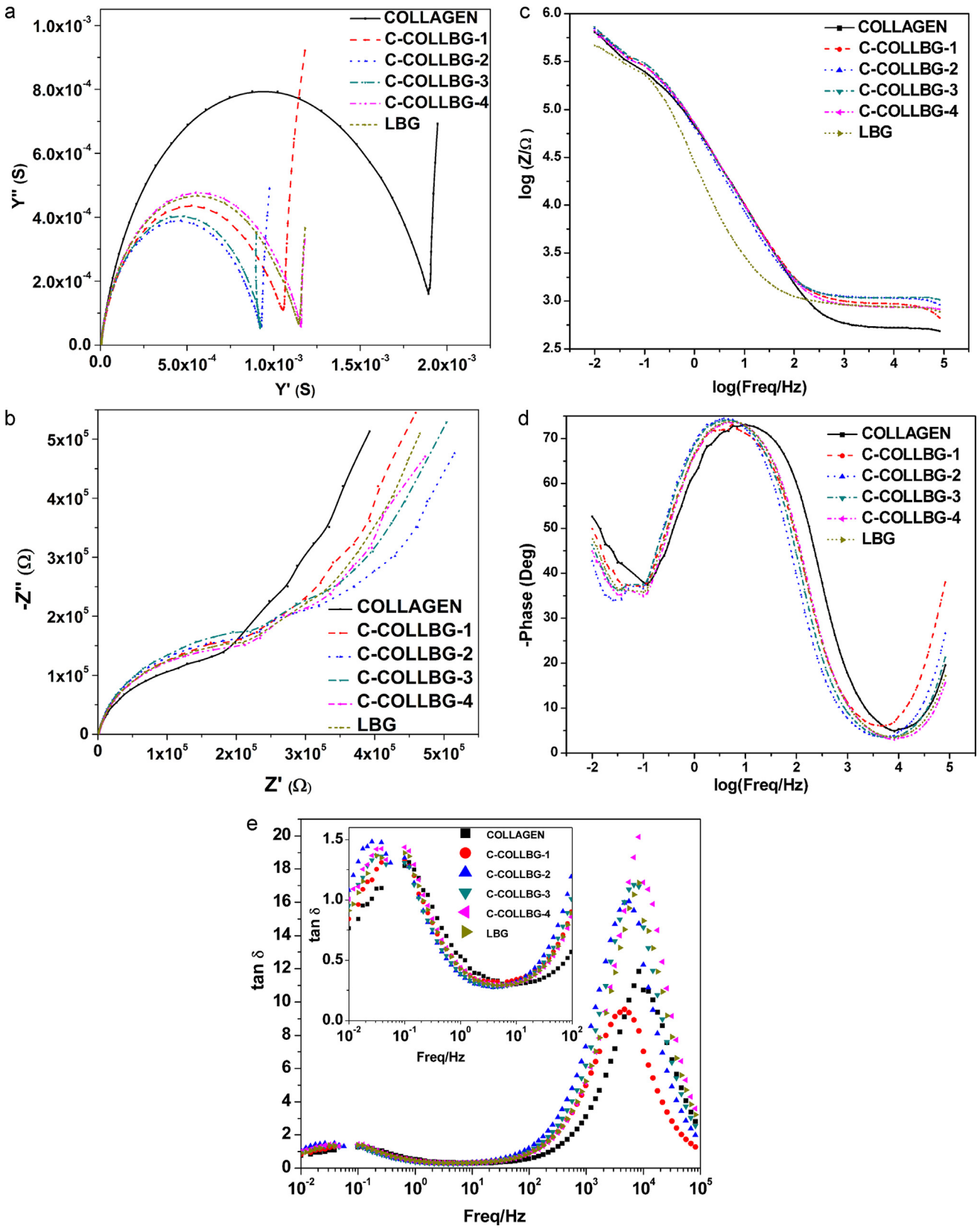

Fig. 5. Dielectric dispersion behaviour of genipin crosslinked collagen–locust bean gum (LBG) composites with different LBG concentration at 298 K. (a) Complex dielectric plane plots for faradaic admittance (real Y' vs. imaginary Y'') measurements. (b) Nyquist plots for faradaic impedance measurements (real Z' vs. imaginary Z''). (c) Frequency evolution of the impedance (Z) in log–log graph (d) Frequency variation of the phase angle in a semi-log graph. (e) Frequency evolution of the energy loss tangent/dissipation factor with different LBG concentrations.

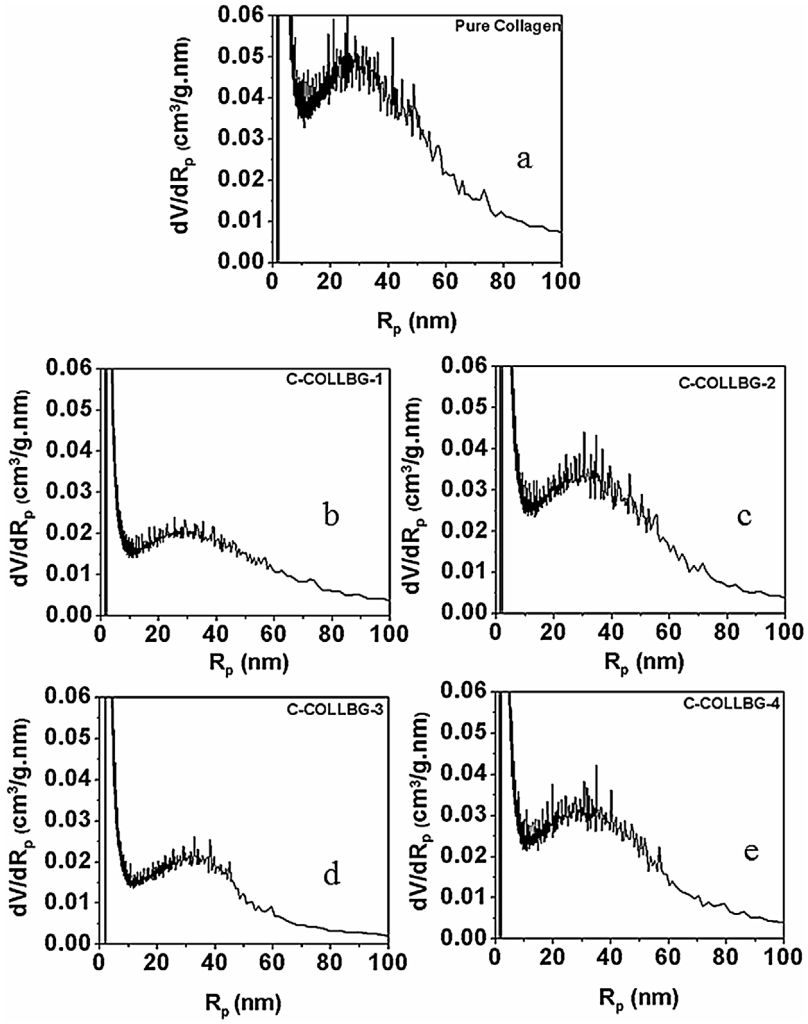

Fig. 6. The pore size distribution of genipin crosslinked collagen–locust bean gum (LBG) composites with different LBG concentration. [collagen] = 0.5 μM: [Locust bean gum] = 0.025–1 μM. Temperature = 233–283 K, rate of increase of temperature = 1 K/min.

rotational potential energy barrier. The peptide groups CONH present in the polypeptide chain behaves like a dipole due to the delocalisation of π electrons, causing dipole–dipole interaction between collagen and LBG. Apart from covalent and hydrogen bond, weak forces between LBG and collagen might result in hydrophilic and hydrophobic interactions. Influence of weak force at fibril level plays a vital role in shifting nucleation centers in monomeric collagen. These forces play a crucial role in stabilization of collagen against heat and enzyme. A complex mixture of hydrophobic, hydrophilic, or charged moieties interfere with the cooperative rearrangement of the hydrogen-bond network of water at collagen–LBG–genipin interfaces.

Multiple hydroxyl groups of LBG involve in noncovalent interaction with the side chain amino groups of collagen. The interatomic forces between LBG and collagen are induced and transient dipoles. The carboxymethyl functionality in the genipin can covalently bind with amino groups of collagen. It is likely that LBG may also be involved in noncovalent hydrogen bonding with the genipin. The bond formation alters the water structure around the functional group, which reorients around the peptide bond. In this case, LBG and genipin alter the hydrophilic interaction between the triple helix, signifying the rearrangement of structural water around the charged amino acid, leading to decrease in the mobility of side chains due to enhancement of the hydrogen bonding network with water and hydroxyproline.

Table 1
Maximum peak frequency value and maximum dissipation factor for C-COLLBG composites with different LBG concentration.

Sample	Max. peak frequency (Hz)	Max. dissipation factor tan δ
Collagen	8558	11.87
LBG	8756	17.18
C-COLLBG-1	4826	9.58
C-COLLBG-2	5684	160.54
C-COLLBG-3	7125	17.104
C-COLLBG-4	8756	19.84

3.4. Characterization of pore size and distribution of collagen–LBG composites – thermoporometry

The porosity of the composites were evaluated based on thermoporometry in wet state by differential scanning calorimeter (DSC) considering that the drying process required for nitrogen adsorption–desorption technique or mercury adsorption technique would affect the pore morphology, specific surface area, pore size, and pore volume. From the melting thermograms, quantitative description of porous materials via the pore size distribution can be calculated (Michael, 2005), which indicate not only several important physical parameters, such as mean pore size, total pore volume, and specific surface area, but also, the

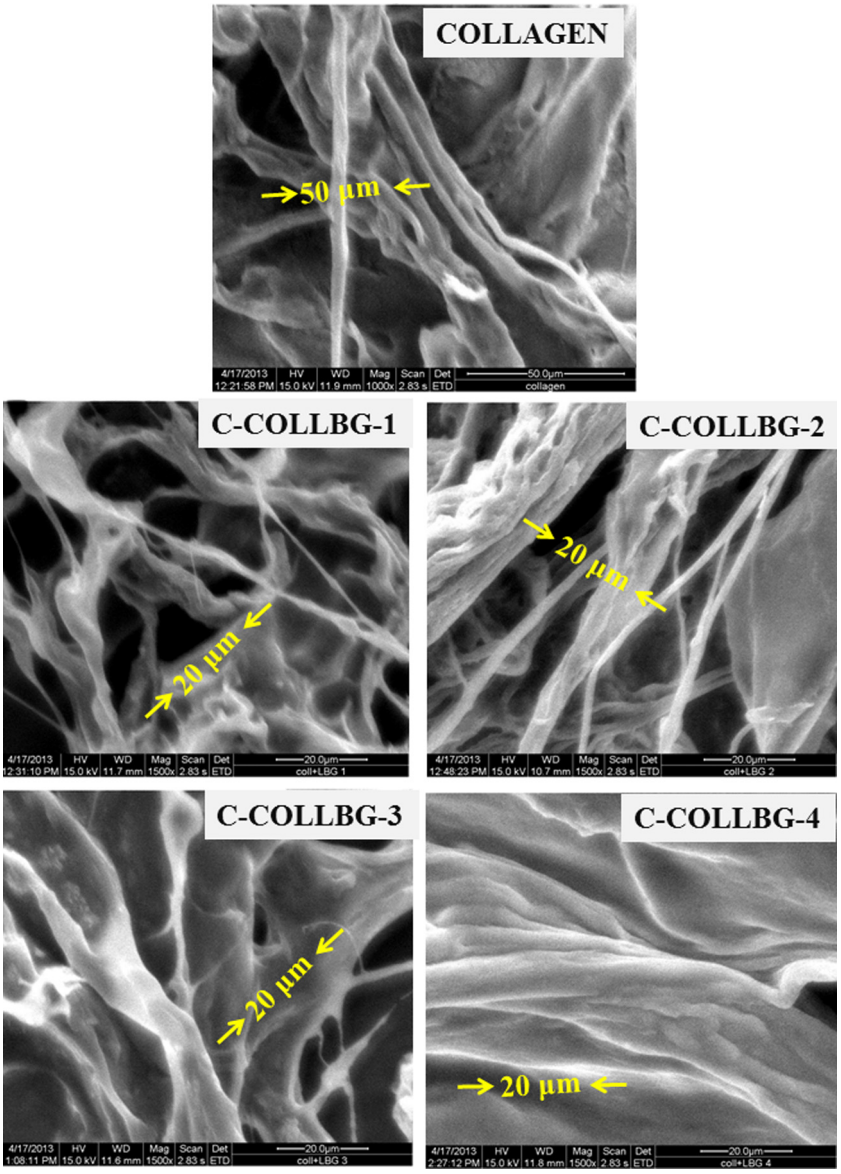

Fig. 7. Porous structure of genipin crosslinked collagen–locust bean gum (LBG) composites with different LBG concentrations as observed using scanning electron microscopy.

shape of distribution provides an additional perspective. The pore size distribution of C-COLLBG is shown in Fig. 6. The shift in melting phase transition of the water confined within a pore of collagen–LBG composite reveals the change in the thermodynamic behaviour from unbound water indicating significant variations in pore size distributions with the various concentration of locust bean gum. Pure collagen has large number of pores in the range of 10–55 nm. The magnitude of the shift of phase transition demonstrates that for [LBG]/[Collagen] = 0.5, pores are distributed in the higher nanometer range (10–50 nm) with a lower pore size distribution indicating presence of less number pores. At [LBG]/[Collagen] = 1, there is an increase in pore population with the decrease in pore sizes (10–40 nm). This implies that the pore network appears to become more closed with large number of pores. Reduction in pore population as well as pore sizes for [LBG]/[Collagen] = 1.5, followed by an increase in pore sizes and pore population at [LBG]/[Collagen] = 2 is observed. Change in dynamic behaviour of water at the collagen–LBG–genipin interfaces results in reorientation of water molecules. The hydration dynamics of the water can be correlated with the formation and breaking of collagen–water, water–water hydrogen bonds. The change in percolation of water–water H-bond network throughout the whole collagen surface is dependent on the LBG concentration. This result is concordant with the above mentioned studies.

3.5. Morphological characterization

The surface morphology of C-COLLBG composites were investigated using scanning electron microscopic (SEM) technique. The morphology of composites magnified at 1500× and morphology of pure collagen magnified at 1000× reveals that an extensive porous network is present as shown in Fig. 7. These mesopores formation might be due to the interaction of collagen with LBG surface by close proximity, thereby allowing noncovalent interactions between them. Less porous nature of the composites at higher LBG concentration might be attributed to the surface deposition of LBG. This interconnected mesoporous architecture of the composites bear a resemblance to that of extracellular matrix structure. This concentration dependent porous architecture of the composites is concordant with physicochemical characteristics studied.

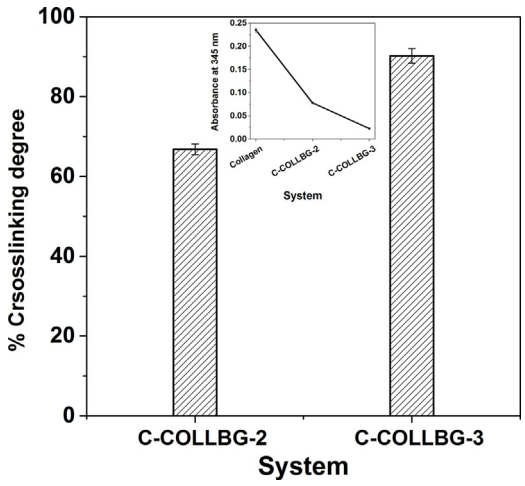

Fig. 8. The crosslinking degree of collagen–LBG composites crosslinked via genipin with different LBG amount.

3.6. Degree of crosslinking by genipin

The unreacted-amino groups of lysine in pure and genipin crosslinked collagen–LBG composite solution react with TNBS to form a soluble complex. The results of the TNBS assay (2,4,6-trinitrobenzenesulfonic acid) shown in Fig. 8 indicate the crosslinking degree of genipin in the collagen–LBG composites. In determining the degree of crosslinking, it has been assumed that each lost amine group participates in an intra- or intermolecular cross-linking reaction of collagen. The degree of crosslinking reaches up to 90% as LBG concentration increases. The addition of genipin causes a loss of free ε-amino groups due to the interaction of —NH_2 groups on the side chains of collagen macromolecules and to form inter- and intra-molecular covalent bonds. Higher crosslinking degree at higher concentration of LBG suggests the dependency of free —NH_2 groups of collagen side chains with LBG as —OH groups of LBG blocks the free —NH_2 groups.

4. Conclusions

This study focuses on the understanding of the effect of LBG and genipin on intra- and intermolecular noncovalent as well as covalent bond formation leading to the structural and stability of collagen. The surface properties of the collagen —LBG based composites provide details about its porous nature, which can help in designing of suitable biomaterial. The influence of such co-solutes on the interfacial behaviour and clustering of bound water of collagen depends on their polarity, amount of components as well as textural features of the materials. The SEM analysis clearly indicates the structural changes in the morphology of LBG—genipin interacted collagen when compared with that of native collagen. Modification of hydration pattern of native collagen will be a step towards the development of material for diverse biomedical applications with reduced antigenicity.

Acknowledgements

Ivy Kanungo acknowledges with thanks to CSIR for providing senior research fellowship. The authors thank CSIR for funding under the Suprainstitutional Project–S&T Revolution in Leather with a Green Touch (CSC0201).

Appendix A. Supplementary data

Supplementary data associated with this article can be found, in the online version, at http://dx.doi.org/10.1016/j.carbpol.2013.12.051.

References

Cerqueira, M. A., Souza, B. W. S., Simões, J., Teixeira, J. A., Domingues, M. R. R. M., Coimbra, M. A., et al. (2011). Structural and thermal characterization of galactomannans from non-conventional sources. *Carbohydrate Polymers*, *83*(1), 179–185.

Chandrakasan, G., Torchia, D. A., & Piez, K. A. (1976). Preparation of intact monomeric collagen from rat tail tendon and skin and the structure of the nonhelical ends in solution. *Journal of Biological Chemistry*, *251*, 6062–6067.

Dakia, P. A., Wathelet, B., & Paquot, M. (2007). Isolation and chemical evaluation of carob seed germ. *Food Chemistry*, *102*, 1368–1374.

Desmet, T., Morent, R., Geyter, N. D., Leys, C., Schacht, E., & Dubruel, P. (2009). Nonthermal plasma technology as a versatile strategy for polymeric biomaterials surface modification: A review. *Biomacromolecules*, *10*(9), 2351–2378.

Dionisio, M., & Grenha, A. (2012). Locust bean gum: Exploring its potential for biopharmaceutical application. *Journal of Pharmacy and Bioallied Sciences*, *4*(3), 175–185.

Fathima, N. N., Baias, M., Blumich, B., & Ramasami, T. (2010). Structure and dynamics of water in native and tanned collagen fibers: Effect of crosslinking. *International Journal of Biological Macromolecules*, *47*, 590–596.

Fathima, N. N., Balaraman, M., Rao, J. R., & Nair, B. U. (2003). Effect of zirconium (IV) complexes on the thermal and enzymatic stability of type I collagen. *Journal of Inorganic Biochemistry*, *95*, 47–54.

Fathima, N. N., Balaraman, M., Rao, J. R., Nair, B. U., & Ramasami, T. (2004). Interaction of aldehydes with collagen: Effect on thermal, enzymatic and conformational stability. *International Journal of Biological Macromolecules*, *34*, 241–247.

Fathima, N. N., Bose, M. C., Rao, J. R., & Nair, B. U. (2006). Stabilization of type I collagen against collagenases (type I) and thermal degradation using iron complex. *Journal of Inorganic Biochemistry*, *100*(11), 1774–1780.

Fathima, N. N., Pradeepkumar, M., Rao, J. R., & Nair, B. U. (2010). A DSC investigation on the changes in pore structure of skin during leather processing. *Thermochimica Acta*, *501*, 98–102.

Farrist, S., Song, J., & Huang, Q. (2009). Alternative reaction mechanism for the crosslinking of gelatin with glutaraldehyde. *Journal of Agricultural & Food Chemistry*, *58*(2), 998–1003.

Friess, W., & Lee, G. (1996). Basic thermoanalytical studies of insoluble collagen matrices. *Biomaterials*, *17*, 2289–2294.

Jafarpour, G., Roig, F., Dantras, E., Boudet, A., & Lacabanne, C. (2009). Influence of water on localized and delocalized molecular mobility of cellulose. *Journal of Non-Crystalline Solids*, *355*(34–36), 1669–1672.

Jayakumar, G. C., Swarna, V. K., Purna Sai, K., Chandrasekaran, B., Rao, J. R., & Nair, B. U. (2012). Scleraldehyde as a stabilizing agent for collagen scaffold preparation. *Carbohydrate Polymers*, *87*, 1482–1489.

Kaity, S., & Ghosh, A. (2013). Carboxymethylation of locust bean gum: Application in interpenetrating polymer network microspheres for controlled drug delivery. *Industrial & Engineering Chemistry Research*, *52*(30), 10033–10045.

Kaity, S., Isaac, J., & Ghosh, A. (2013). Interpenetrating polymer network of locust bean gum poly (vinyl alcohol) for controlled release drug delivery. *Carbohydrate Polymers*, *94*, 456–467.

Kaity, S., Isaac, J., Mahesh Kumar, P., Bose, A., Wong, T. W., & Ghosh, A. (2013). Microwave assisted synthesis of acrylamide grafted locust bean gum and its application in drug delivery. *Carbohydrate Polymer*, *98*(1), 1083–1094.

Kaminski, K., Kaminska, E., Ngai, K. L., Paluch, M., Wlodarczyk, P., Kasprzycka, A., et al. (2009). Identifying the origins of two secondary relaxations in polysaccharides. *Journal of Physical Chemistry B*, *113*, 10088–10096.

Kandamchira, A., Kanungo, I., & Fathima, N. N. (2012). Dielectric behaviour and conformational stability of collagen on interaction with DNA. *International Journal of Biological Macromolecules*, *51*, 635–639.

Kanungo, I., Chellappa, N., Fathima, N. N., & Rao, J. R. (2011). Calorimetric analysis of gelatine – glycosaminoglycans blend system. *International Journal of Biological Macromolecules*, *49*, 289–296.

Kanungo, I., Fathima, N. N., Rao, J. R., & Nair, B. U. (2013a). Hydration dynamics of collagen/PVA composites: Thermoporometric and impedance analysis. *Materials Chemistry and Physics*, *140*, 357–364.

Kanungo, I., Fathima, N. N., Rao, J. R., & Nair, B. U. (2013b). Influence of PCL on the material properties of collagen based biocomposites and in vitro evaluation of drug release. *Materials Science & Engineering C*, *33*, 4651–4659.

Manikoth, R., Kanungo, I., Fathima, N. N., & Rao, J. R. (2012). Dielectric behaviour and pore size distribution of collagen–guar gum composites: Effect of guar gum. *Carbohydrate Polymers*, *88*, 628–637.

Marzec, E., & Warchol, W. (2005). Dielectric properties of a protein – water system in selected animal tissues. *Bioelectrochemistry*, *65*, 89–94.

Michael, R. L. (2005). Thermoporometry by differential scanning calorimetry: Experimental considerations and applications. *Thermochimica Acta*, *433*, 27–50.

Nishi, C., Nakajima, N., & Ikada, Y. (1995). In vitro evaluation of cytotoxicity of diepoxy compounds used for biomaterial modification. *Journal of Biomedical Material Research*, *29*, 829–834.

O'Brien, F. J., Harley, B. A., Yannas, I. V., & Gibson, L. J. (2005). The effect of pore size on cell adhesion in collagen-GAG scaffolds. *Biomaterials*, *26*, 433–441.

Parvathy, K. S., Susheelamma, N. S., Tharanathan, R. N., & Gaonkar, A. K. (2005). A simple non-aqueous method for carboxymethylation of galactomanans. *Carbohydrate Polymer*, *62*, 137–141.

Prajapatia, V. D., Jani, G. K., Moradiya, N. G., Randeria, N. P., Nagar, & Bhanu, J. (2013). Locust bean gum: A versatile biopolymer. *Carbohydrate Polymers*, *94*, 814–821.

Ramachandran, G. N. (1967). *Treatise on collagen*. London: Academic Press.

Rinaudo, M. (2008). Main properties and current applications of some polysaccharides as biomaterials. *Carbohydrate Polymers*, *57*, 397–430.

Samouillan, V., Lamure, A., & Lacabanne, C. (2000). Dielectric relaxations of collagen and elastin in the dehydrated state. *Chemical Physics*, *255*, 259–271.

Samouillan, V., Lamure, A., Maurel, E., Dandurand, J., Lacabanne, C., Ballarin, F., et al. (2000). Characterisation of elastin and collagen in aortic bioprothese. *Medical & Biological Engineering & Computing*, *38*, 226–231.

Sen, M., & Erboz, E. N. (2010). Determination of critical gelation conditions of [kappa]-carrageenan by viscosimetric and FT-IR analyses. *Food Research International*, *43*(5), 1361–1364.

Turquois, T., Acquistapace, S., Vera, F., & Welti, D. H. (1996). Composition of carrageenan blends inferred from 13C-NMR and infrared spectroscopic analysis. *Carbohydrate Polymers*, *31*(4), 269–278.

Wang, J., & Somasundaran, P. (2007). Study of galactomannose interaction with solids using AFM, IR and allied techniques. *Journal of Colloid and Interface Science*, *309*, 373–383.

Woessner, J. F., Jr. (1961). The determination of hydroxyproline in tissue and protein samples containing small proportions of this imino acid. *Archives of Biochemistry and Biophysics*, *93*, 440–447.

Xu, X., Li, B., Kennedy, J. F., Xie, B. J., & Huang, M. (2007). Characterization of konjac glucomannan–gellan gum blend films and their suitability for release of nisin incorporated therein. *Carbohydrate Polymers*, *70*, 192–197.

Yalçın, O., Coşkun, R., Okutan, M., & Öztürk, M. (2013). Comparison effects and dielectric properties of different dose methylene-blue-doped hydrogels. *Journal of Physical Chemistry B*, *117*(30), 8931–8938.

Yoo, J. S., Kim, Y. J., Kim, S. H., & Choi, S. H. (2011). Study on genipin: A new alternative natural crosslinking agent for fixing heterograft tissue. *The Korean Journal of Thoracic and Cardiovascular Surgery*, *44*(3), 197–207.

Zhou, J., Zhang, J., Ma, Y., & Tong, J. (2008). Surface photocrosslinking of corn starch sheets. *Carbohydrate Polymers*, *74*(3), 405–410.